ISSN 1392-1207. MECHANIKA. Vol. 29, No. 5, 2023: 387–394

Real-Time Energy Consumption Sensing System in SMT Intelligent Workshop

Fengque PEI*,, Zhi LI*,**, Wei DI*, Song MEI***, Haojie SONG*****

**College of Mechanical and Electrical Engineering, Hohai University, Changzhou, 213000, China, E-mail: FQ_Pei@163.com*

***Changzhou Key Laboratory of Intelligent Manufacturing Technology and Equipment, Hohai University, Changzhou, 213000, China, E-mail: 221619010043@hhu.edu.cn*

****Nanjing Institute of Agricultural Mechanization, Ministry of Agriculture and Rural Affairs, Nanjing, 210014, China, E-mail: meisong@caas.cn*

*****Nanjing Research Institute of Electronic Engineering, Nanjing, 210007, China, E-mail: 15051891899@163.com*

https://doi.org/10.5755/j02.mech.32129

1. Introduction

China has the most quantities of the manufacturing systems and mechanical equipment all around the world, and the total energy consumption is the largest. While the energy utilization is lower than 30%. In 2019, the carbon dioxide generated by China reaches to 10 billion tons, making up to 30% in the whole world (33.1 billion tons). What's worse, it still maintains an annual growth of about 1.5%. The US has an annual emission of 4.8 billion tons, and the rate continues to decline both in US and EU. On the other hand, from carbon peaking to carbon neutrality, it is 43 years from 2007 to 2050 planed by US, and it is 71 years for EU. While it is only 30 years for China [1]. So, ensure the "carbon peaking and carbon neutrality" goal is a crucial part for China with good performance, low cost and limited time. The nature of energy consumption sensing and energy efficiency controlling provide great insights about concept of innovation, coordination, greenness, openness and sharing [2], helping to prioritize efforts for reducing the carbon dioxide emissions per unit of GDP [3].

The primary idea of energy consumption [4-5] and energy efficiency is mainly divided into two levels. The workshop-level mainly includes the modeling, the optimization and the evaluation of energy consumption and energy efficiency in the manufacturing systems. For example, Liu [6] put forward four characteristics of energy consumption state and energy efficiency evaluation: multi-energy source characteristics and hierarchical distribution characteristics, energy consumption process and transient energy efficiency complex variability, and product life cycle process characteristics. He [7] analyzed the energy consumption characteristics of the processing task scheduling oriented to the flexible process route of the mechanical workshop based on the influence characteristics of the flexible process route of the mechanical workshop task on the energy consumption of the mechanical workshop scheduling, processing completion time, machine tool load as the goal of energy-saving scheduling model, and further proposed an improved Q-learning algorithm to solve the model to obtain its Pareto solution, thereby improving the energy efficiency of the machine shop. Zhang [8] established an energy efficient flexible job shop scheduling problem model by considering the transportation time in response to the energy-saving operation requirements of flexible job shops, and used genetic algorithms to solve the model. It also reflects the method of realizing energy-saving operation of workshop manufacturing through machine tool selection and process sequencing. He [9-10] formed a preheating-quenching model and a preheating-tempering model for the forging preheating and heating workshop. The optimization model with the capacity difference as the main function was carried out for the typical paradigm of energy saving and consumption reduction in the forging workshop.

Additionally, equipment-level energy-saving design is another major approach [11]: The Fraunhofer Institute of Machine Tool and Forming Technology in Germany proposes an energy efficiency control model with energy autonomy and zero emissions. Japan Mori Seiki modeled the multi-source energy consumption of machine tools and proposed a method for processing energy consumption. Massachusetts Institute of Technology analyzed the motor energy flow [12] to reveal device-level energy distribution. Zhang [13] proposed a new bond graph method for modelling the dynamics characteristics and energy consumption of the spindle system of a CNC machine tool to comprehensively consider the energy consumption and dynamics characteristics of the mechanical transmission of the spindle system. He [14] estimated the machining feature energy consumption under flexible machining configurations. This method can help manufacturers to select optimal energy-efficient machining configurations for performing workpieces and provide designers with knowledge of energy consumption to conduct energy-saving design of features.

After the above literature review, due to the complex types of equipment and large energy nodes, the energy consumption research mostly stays at the factory or workshop level and facing the following problems: 1) Multi-level, multi-source energy consumption increase the modeling complexity [15]. 2) The real-time responsiveness of the energy efficiency sensing network is challenged by the large number of energy sensing nodes and the group control performance requirements of logistics /distribution equipment. 3) The delayed transmission data cannot form an effective online energy efficiency evaluation and optimization control. These limitations greatly hinder the fine control of energy efficiency in intelligent workshops.

Therefore, the primary arm of this research is to investigate how an energy consumption architecture im-

plement the device-level energy consumption sensing and workshop-level energy consumption modeling in the SMT production lines. This paper presents a more detailed enhancement of energy sensing and modeling method. The rest of the paper is organized as follows: In second section, the overall architecture of energy consumption sensing and modelling are described. The third section introduces the detailed implements of the device -level real-time energy consumption sensing technology. The fourth section presents the workshop-level energy consumption modeling in a general way and the fifth section summaries the paper and gives some consideration about the future work.

2. The overall architecture of the real-time energy consumption system

According to energy consumption has some important fields of application and it is widely discussed. This section describes an overall architecture of the real-time energy consumption system in a general way and argues for its characteristic when applied in SMT production lines.

2.1. The SMT production lines

The SMT production lines have the characteristics of high production efficiency and strong flexibility. And the SMT orders have the characteristics of small batch, high frequency, and large total amount. Therefore, the SMT production lines often show cluster characteristics. For example, AKM Electronic Technology Group, one of the leading enterprises in the SMT industry, has formed a cluster of nearly 40 production lines. This cluster has a high degree of customization and the non-standard process is about 30, involving more than 100 sets of heterogeneous equipment, which is a typical equipment-intensive production line cluster. This study takes the SMT production line cluster as an example. A detailed single SMT production line is shown in Fig. 1. From the beginning, the flexible printed circuit (FPC) is transported by the AGV to the feeding machine and combines with the fixtures. The solder paste is printed in the printing machine and the checked by the solder paste inspection machine (SPI). After the inspection of the thickness & area and other quality parameters, the FPC is delivered to the chip mounter to weld with the NX and some other electronic devices. Then, it is reflowed soldering process. The automated optical inspection (AOI) is introduced to inspect the pose position and the welding quality. Most of the production lines are U-shape, where AGV transmission is carried out to the glue dispenser to package the NX pin. And then, the ultraviolet curing machine (UV) and vacuum baking machine is introduced to accelerate the solidification process. The X-ray inspection station is carried out to indicate the air bubbles, pin deformation, etc. Finally, the manually check station is used to ensure the outlooking and conductivity. Among them, the failed piece of each inspection will be picked out and marked as NG, and then repaired by workers. The cluster process is similar to the above process.

2.2. The overall architecture of the real-time energy consumption system in SMT production lines

The overall architecture is divided into two categories. The former is the device-level energy consumption sensing technology with the complex working condition machine whose power is unknown, such as robotic or AGVs. The power is unknown under multi working states. The energy consumption sensing technology based on mutual inductance is discussed, and the data will be transmitted to the data center over RS485. The second type is the equipment with certain power. The working state can be divided into several states such as shutdown, preheating, and working. The power in different states is marked in the nameplate. A multi-granularity production line energy consumption calculation paradigm (3-matrix method) is put forward. The paradigm is shown in Fig. 2.

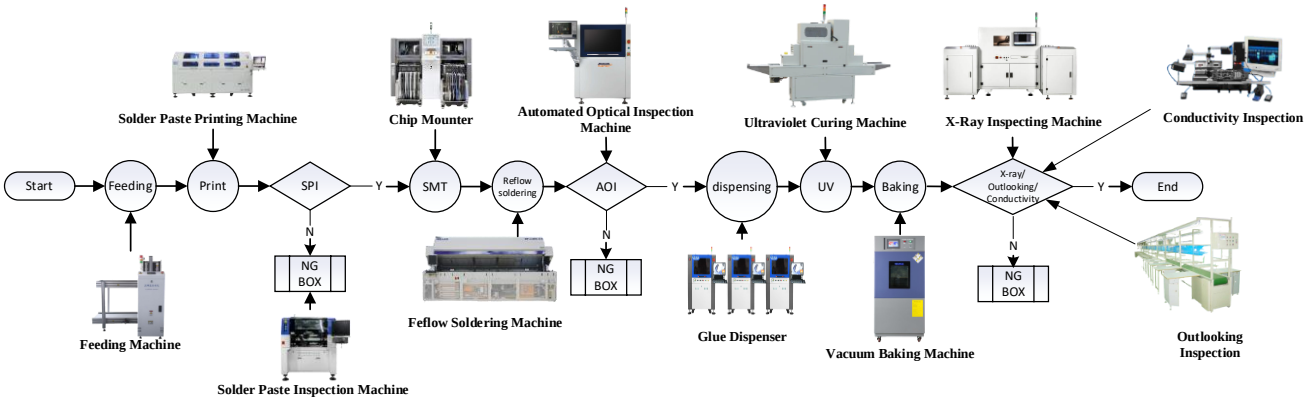

Fig. 1 SMT production line and basic process

3. Device-level energy consumption real-time sensing technology based on mutual inductance

Section 3 demonstrates the detailed implementation of the energy consumption real-time sensing technology based on mutual inductance in the device-level for the multi working condition machines whose power is unknown.

3.1. Robot energy flow analysis

In order to understand the efficiency of a robot when performing a series of standard operations, the energy flow is analyzed as shown in Figs. 3 and 4.

The energy consumption P_A is generated by the robot for each command, part of which is the mechanical energy consumption P_{out} and the other part P_{loss} is the lost in the friction. The total energy consumption is P_{all}:

$$P_{all} = P_{out} + P_{loss}. \quad (1)$$

The efficiency of each stage in the palletizing op-

eration is shown below:

$$\eta = \frac{E_{part_i}}{E_{out}} \times 100\% \quad , \quad E_{out} = \sum_{i}^{n} E_{part_i} \tag{2}$$

where: E_{part_i} is energy consumption, for performing a certain phase of the palletizing operation; E_{out} is the total output energy consumption, J of the palletizing operation.

The energy consumption of each stage depends on the power of this stage. Since the current change in real time, the power will also change in real time with the current. So E_{out} can be expressed as:

$$E_{out} = \sum_{i}^{n} \int_{t_{is}}^{t_{ie}} P_A dt, \tag{3}$$

where: t_{is} the starting time, s of the *ith* operation stage; t_{ie} the ending time, s of the *ith* operation. The friction loss P_{loss} can be expressed:

$$P_{loss} = \sum_{i}^{n} f_i(\omega_i)\omega_i, \tag{4}$$

where: ω_i the angular velocity, rad/s.

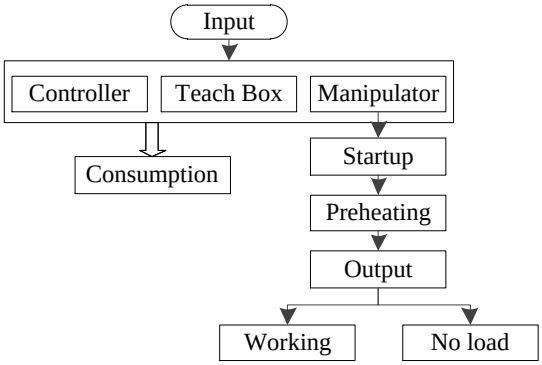

Fig. 2 Robot energy flow

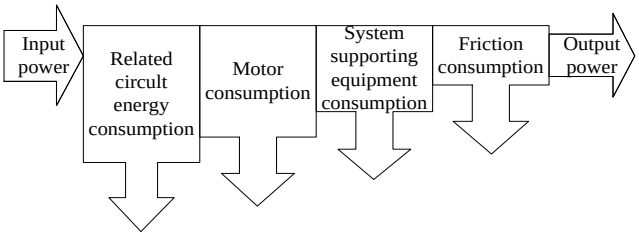

Fig. 3 Energy consumption flow

The auxiliary energy consumption in actual working conditions of robots is as follows:

$$E_a = \sum_{i=1}^{n_a} \int_{t_{ais}}^{t_{aie}} P_A dt, \tag{5}$$

where: E_a auxiliary energy consumption of robot, J; t_e the number of auxiliary periods; t_{ais} the starting time, s of the *ith* auxiliary period; t_{aie} the ending time, s of the *ith* auxiliary period.

The total energy consumption of the robot under actual operation conditions is:

$$E_T = \int_{t_s}^{t_e} P_A dt, \tag{6}$$

where: E_T the total energy consumption of actual loop, J; t_s the starting time of the actual loop, s; t_e the ending time of the actual loop, s.

3.2. Real-time energy consumption sensing

Firstly, the standard loop and the actual loop of the robot are built up.

In a standard loop, the real-time energy consumption E_S can be divided into the operation energy consumption and the segment energy consumption:

$$E_f = \sum_{i=1}^{n} \int_{t_{sns}}^{t_{sne}} P_A dt + \sum_{i=1}^{m} \int_{t_{sms}}^{t_{sme}} P_A dt, \tag{7}$$

where: $\sum_{i=1}^{n} \int_{t_{sns}}^{t_{sne}} P_A dt$ the operation energy consumption, J; n the number of robot operations; t_{sns} the starting time, of the operation n, s; t_{sne} the ending time, s corresponding to t_{sns}; $\sum_{i=1}^{m} \int_{t_{sms}}^{t_{sme}} P_A dt$ the segmented energy consumption, J; m number of segments; t_{sms} the starting time, s of a segment m; t_{sme} the ending time, s corresponding to t_{sms}.

In this research, the operation energy consumption is E_{work}. The segment energy consumption E_{part} includes the startup energy consumption E_{start}, the preheating energy consumption $E_{preheat}$ the waiting energy consumption E_{wait}. While the auxiliary energy consumption E_A and the abnormal energy consumption E_F are not considered in the standard loop. So:

$$E_s = E_{work} + E_{start} + E_{preheat} + E_{wait}. \tag{8}$$

In actual loop, the real-time energy consumption E_T can be divided into the operation energy consumption and the segment energy consumption also:

$$E_T = \sum_{i=1}^{n} \int_{t_{ans}}^{t_{ane}} P_A dt + \sum_{i=1}^{m} \int_{t_{ams}}^{t_{ame}} P_A dt + \sum_{i=1}^{j} \int_{t_{ajs}}^{t_{aje}} P_A dt, \tag{9}$$

where: $\sum_{i=1}^{n} \int_{t_{ans}}^{t_{ane}} P_A dt$ the operation energy consumption, J; n the number of operations; t_{ans} the starting time, s of a operation n; t_{ane} the ending time, s corresponding to t_{ans}. $\sum_{i=1}^{m} \int_{t_{ams}}^{t_{ame}} P_A dt$ the segmented energy consumption, J; m the number of segments; t_{ams} the starting time of segment m, s; t_{ame} the ending time, s corresponding to t_{ams}. $\sum_{i=1}^{j} \int_{t_{ajs}}^{t_{aje}} P_A dt$ auxiliary energy consumption, J; j number of auxiliaries; t_{ajs} the starting time of a auxiliary j, s; t_{aje} the ending time, s corresponding to t_{ajs}.

In this research, the operation energy consumption is E_{work}. The segment energy consumption E_{part} includes the startup energy consumption E_{start}, the preheating energy consumption $E_{preheat}$ and the waiting energy con-

sumption E_{wait}, the auxiliary energy consumption is E_a, and the abnormal energy consumption E_F is not considered in the actual loop. So:

$$E_T = E_{work} + E_{start} + E_{preheat} + E_{wait} + E_A \quad (10)$$

In the palletizing operation, and the energy consumption in the startup phase and the preheating phase are shown in Table 1.

Table 1

The current in startup and preheating phase

Time, s	Current, mA	Time, s	Current, mA	Time, s	Current, mA
0.2	2265.43	2.0	2271.11	3.8	2269.15
0.4	2264.47	2.2	2266.41	4.0	2267.94
0.6	2274.87	2.4	2265.50	4.2	748.33
0.8	2269.81	2.6	2265.28	4.4	738.17
1.0	2273.30	2.8	2264.72	4.6	749.82
1.2	2264.86	3.0	2265.90	4.8	746.65
1.4	2277.01	3.2	2275.02	5.0	750.66
1.6	2276.26	3.4	2271.95	5.2	105.30
1.8	2275.36	3.6	2272.62	5.4	106.13

The sum of the startup energy consumption and preheating energy consumption is 3723.54 J.

The working energy consumption in standard loop is shown in Table 2. And the total is 4642.74 J.

Table 2

The current in working phase of the standard loop

Time, s	Current, mA	Time, s	Current, mA	Time, s	Current, мА
0.2	806.80	2.8	872.45	5.4	105.53
0.4	820.10	3.0	874.00	5.6	108.13
0.6	791.66	3.2	901.96	5.8	105.89
0.8	815.50	3.4	825.27	6.0	781.10
1.0	801.73	3.6	818.72	6.2	781.55
1.2	-253.81	3.8	802.53	6.4	782.35
1.4	-244.69	4.0	792.78	6.6	782.03
1.6	-261.29	4.2	795.24	6.8	108.75
1.8	105.00	4.4	-311.21	7.0	106.51
2.0	108.82	4.6	-339.36	7.2	107.25
2.2	105.85	4.8	-328.10	7.4	107.44
2.4	106.75	5.0	106.07	7.6	107.87
2.6	107.60	5.2	106.15		

As shown in Table 3, in the actual working loop, the total is 7452.65 J. The auxiliary energy is 1320 J.

Table 3

The current in working phase of the actual loop

Time, s	Current,мА	Time, s	Current, mA	Time, s	Current, mA
0.2	820.80	2.8	874.04	5.4	106.95
0.4	810.77	3.0	902.98	5.6	108.81
0.6	796.53	3.2	882.70	5.8	108.77
0.8	805.91	3.4	824.97	6.0	782.05
1.0	800.23	3.6	825.37	6.2	781.34
1.2	-242.48	3.8	813.99	6.4	780.74
1.4	-258.24	4.0	811.38	6.6	782.52
1.6	-250.39	4.2	801.47	6.8	108.90
1.8	107.92	4.4	-334.08	7.0	105.66
2.0	107.73	4.6	-314.56	7.2	105.04
2.2	107.90	4.8	-334.57	7.4	108.75
2.4	105.29	5.0	106.26	7.6	105.842
2.6	108.63	5.2	108.66		

3.3. The study of energy efficiency

In this study, a gripper is installed on the AUBO-i5 robot. As shown in Fig. 4.

1) Nominal value of operation energy consumption: ten standard loops are carried out and the average result is calculated.

2) The percentage of auxiliary energy consumption:

$$\Delta_a = \frac{E_a}{E_T} \times 100\%. \quad (11)$$

3) Operation energy efficiency coefficient:

$$\Delta = \frac{E_N \times n_T \times \eta}{E_T} \times 100\%, \quad (12)$$

where: Δ the operation energy efficiency coefficient; n_T in the actual loop, the number of tasks completed by the robot; η the pass rate of the robot task in the actual loop.

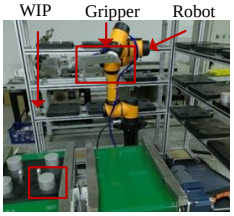

Fig. 4 The AUBO-i5

According to the nominal value of operation energy consumption, 10 results are shown in Table 4.

Table 4

10 result of Energy consumption

Loop No.	Value	Loop No.	Value
E_{S1}	4642.74	E_{S7}	4672.34
E_{S2}	4697.81	E_{S8}	4771.75
E_{S3}	4619.67	E_{S9}	4704.32
E_{S4}	4725.40	E_{S10}	4668.53
E_{S5}	4693.51	E_a	1320
E_{S6}	4718.11	E_T	7452.65

The nominal value is:

$$E_N = \frac{\sum_{i=1}^{10} E_{si}}{10} = 4691.42\text{J}.$$

The auxiliary energy proportional coefficient is:

$$\Delta_a = \frac{E_a}{E_T} \times 100\% = 17.71\%.$$

The number of tasks completed by the robot n_T (100%), and the pass rate η (100%) are taken in, the operation energy efficiency coefficient:

$$\Delta = \frac{E_N \times n_T \times \eta}{E_T} \times 100\% = 62.95\%.$$

4. Workshop-level energy consumption modelling

Section 4 devoted the basic aspects of the pro-

posed multi-granularity production line energy consumption modeling and summarized the implementation elements of 3- matrix (the attribute attributes, power attributes and cumulative timing attributes). The 3-matrix is used to calculate the SMT equipment, process, production line, order and workshop energy consumption.

$$[a]=\begin{bmatrix} a_{1-starting}^{SMT1} & a_{1-dormant}^{SMT1} & a_{1-working}^{SMT1} \\ a_{2-starting}^{SMT1} & a_{2-dormant}^{SMT1} & a_{2-working}^{SMT1} \\ \dots & \dots & \dots \\ a_{i-starting}^{SMTn} & a_{i-doramnt}^{SMTn} & a_{i-working}^{SMTn} \end{bmatrix}. \quad (13)$$

First of all, an attribute attribution matrix (represented as [a] matrix) is constructed, which is a [total×3] matrix, and has a total-dimensions. The 3-dimensional column vector of the matrix represents the three states of the equipment as the Eq. (13). $a_{i-starting}^{SMTn}$ is a Boolean of the SMT production line n device i in the starting phase, "0" indicates not working, and "1" in working. $a_{i-dormant}^{SMTn}$ and $a_{i-working}^{SMTn}$ are also Boolean also, "0" means not in dormancy nor working. "1" is in dormancy or working. $a_{i-starting}^{SMTn}$ and $a_{i-dormant}^{SMTn}$, are mutually exclusive and can be "0" at the same time, which indicates the shutdown state.

Secondly, the power matrix (denoted as [p]) and cumulative timing matrix (denoted as [t]) are:

$$[p]=\begin{bmatrix} p_{1-starting}^{SMT1} & p_{1-dormant}^{SMT1} & p_{1-working}^{SMT1} \\ p_{2-starting}^{SMT1} & p_{2-dormant}^{SMT1} & p_{2-working}^{SMT1} \\ \dots & \dots & \dots \\ p_{i-starting}^{SMTn} & p_{i-dormant}^{SMTn} & p_{i-working}^{SMTn} \end{bmatrix}. \quad (14)$$

The [p] is a static matrix, which records the power of each equipment in each production line in each state. The [t] matrix represents the time to maintain this state and is the cumulative result.

After that, the standard sensing time t is set as the production takt. Therefore, the [t] is:

$$\begin{bmatrix} t_{1-starting}^{SMT1} & t_{1-dormant}^{SMT1} & t_{1-working}^{SMT1} \\ t_{2-starting}^{SMT1} & t_{2-dormant}^{SMT1} & t_{2-working}^{SMT1} \\ \dots & \dots & \dots \\ t_{i-starting}^{SMTn} & t_{i-dormant}^{SMTn} & t_{i-working}^{SMTn} \end{bmatrix} + t \times \begin{bmatrix} a_{1-starting}^{SMT1} & a_{1-dormant}^{SMT1} & a_{1-working}^{SMT1} \\ a_{2-starting}^{SMT1} & a_{2-dormant}^{SMT1} & a_{2-working}^{SMT1} \\ \dots & \dots & \dots \\ a_{i-starting}^{SMTn} & a_{i-dormant}^{SMTn} & a_{i-working}^{SMTn} \end{bmatrix}, \quad (15)$$

The 3-matric is:

$$[E]=\begin{bmatrix} p_{1-starting}^{SMT1} & p_{1-dormant}^{SMT1} & p_{1-working}^{SMT1} \\ p_{2-starting}^{SMT1} & p_{2-dormant}^{SMT1} & p_{2-working}^{SMT1} \\ \dots & \dots & \dots \\ p_{i-starting}^{SMTn} & p_{i-dormant}^{SMTn} & p_{i-working}^{SMTn} \end{bmatrix} \cdot \begin{bmatrix} t_{1-starting}^{SMT1} & t_{1-dormant}^{SMT1} & t_{1-working}^{SMT1} \\ t_{2-starting}^{SMT1} & t_{2-dormant}^{SMT1} & t_{2-working}^{SMT1} \\ \dots & \dots & \dots \\ t_{i-starting}^{SMTn} & t_{i-dormant}^{SMTn} & t_{i-working}^{SMTn} \end{bmatrix}, \quad (16)$$

The "·" means dot product, [E] means the energy consumption.

Finally, a multi-granularity production line energy consumption calculation paradigm can be summarized, as shown in Table 5.

A case study is adapted to make it clearly. It is found that SMT line 1, 2, and 5 have roughly same configuration. The [p], [t] and [a] matrix is shown in Tables 6-8.

Table 5

Energy consumption calculation paradigm of multi-granularity SMT production line

	Index	Formula		Description
Equipment energy consumption	A single device real-time energy consumption, KW	$a_{j-Xnow}^{SMTx} \cdot p_{j-X_{now}}^{SMTx}$	(17)	T – standard sensing time; X – the SMT production line x; j – the jth device; X_{now} – the current working state
	A single device single-state energy consumption, KW	$a_{j-X}^{SMTx} \cdot t_{j-X}^{SMTx} \cdot p_{j-X}^{SMTx}$	(18)	$X \in$ [starting, dormant, working]; t_{j-X}^{SMTx} represents the accumulated time of the state, and real-time data or optional time interval data can be controlled by the range of t_{j-X}^{SMTx} (database multi-table select).
	A single device total energy consumption, KWh	$\sum_{X=starting}^{working} a_{j-X}^{SMTx} \cdot t_{j-X}^{SMTx} \cdot p_{j-X}^{SMTx}$	(19)	As above
Process energy consumption	Multiple devices (units with energy combinations) real-time energy consumption, KWh	$\sum_{j=m}^{n} a_{j-X_{now}}^{SMTx} \cdot p_{j-X_{now}}^{SMTx}$	(20)	j represents the jth device; $j \in [m, n]$, which means that the device contains [m, n], subjects.
	Multiple devices single-state energy consumption, KWh	$\sum_{j=m}^{n} a_{j-X_{now}}^{SMTx} \cdot t_{j-X}^{SMTx} \cdot p_{j-X}^{SMTx}$	(21)	Total energy consumption of [m, n] agents in state X

	Index	Formula		Description
	Multiple devices total energy consumption, KWh	$\sum_{j=m}^{n}\sum_{X=starting}^{working} a_{j-X}^{SMTx}\cdot t_{j-X}^{SMTx}\cdot p_{j-X}^{SMTx}$	(22)	
Production line energy consumption	Single *SMT*, *No*. production line real-time energy consumption, KW	$\sum_{SMTx\in SMT(No.)} a_{j-X_{now}}^{SMTx}\cdot p_{j-X_{now}}^{SMTx}$	(23)	*SMT*, *No*. represents a certain SMT production line; $SMTx\in SMT$, *No.* represents all equipment belonging to the *SMT*, *No*. production line
	Single *SMT*, *No*. production line single-state energy consumption, KWh	$\sum_{SMTx\in SMT(No.)} a_{j-X}^{SMTx}\cdot t_{j-X}^{SMTx}\cdot p_{j-X}^{SMTx}$	(24)	
	Single *SMT*, *No*. production line total energy consumption, KWh	$\sum_{SMTx\in SMT(No.)}\sum_{X=starting}^{working} a_{j-X}^{SMTx}\cdot t_{j-X}^{SMTx}\cdot p_{j-X}^{SMTx}$	(25)	
Workshop energy consumption	Workshop real-time energy consumption, KW	$\sum a_{j-X_{now}}^{SMTx}\cdot p_{j-X_{now}}^{SMTx}$	(26)	$\sum$ represents all the equipment in the workshop, or represents all the elements in the 3-matrix table.
	Workshop single-state energy consumption, KWh	$\sum a_{j-X}^{SMTx}\cdot t_{j-X}^{SMTx}\cdot p_{j-X}^{SMTx}$	(27)	
	Workshop total energy consumption, KWh	$\sum\sum_{X=starting}^{working} a_{j-X}^{SMTx}\cdot t_{j-X}^{SMTx}\cdot p_{j-X}^{SMTx}$	(28)	

Table 6

The [*p*] matrix of the SMT production line 1, 2, 5

Machine No.	Equipment description	Starting, KW	Dormancy, KW	Working, KW
SMT-1	Punch machine	35	0.8	8.5
SMT-2	UV	26	0.8	6.5
SMT-3	AOI	16	0.8	3
SMT-4	High precision dual screen printer machine	24	0.8	4.7
SMT-5	Automatic solder pastes printing machine	7	0.5	1.5
SMT-6	Fully automatic special-shaped chip mounter machine	13	0.8	2.5
SMT-7	Modular high-speed multi-function machine	48	0.8	10
SMT-8	Fully automatic offline inkjet printer	31	0.8	4.8
SMT-9	Automatic chip mounter	28	0.8	5
SMT-10	10 Zone N2 dual rail reflow soldering machine	83	1	16.5
SMT-11	Glue dispenser	12	0.5	2.3
SMT-12	Printing machine	8	0.5	1.5

Table 7

The [*t*] matrix of the SMT production line 1, 2, 5

Machine No.	Starting, h	Dormancy, h	Working, h	Machine No.	Starting, h	Dormancy, h	Working, h
SMT1-1	0.28	1.16	6.57	SMT2-7	0.25	1.78	5.97
SMT1-2	0.23	1.17	6.60	SMT2-8	0.11	1.82	6.08
SMT1-3	0.07	1.19	6.74	SMT2-9	0.03	1.83	6.13
SMT1-4	0.17	1.18	6.66	SMT2-10	0.77	1.66	5.57
SMT1-5	0.03	1.20	6.78	SMT2-11	0.03	1.83	6.14
SMT1-6	0.03	1.20	6.77	SMT2-12	0.04	1.83	6.13
SMT1-7	0.25	1.16	6.59	SMT3-1	0.28	5.33	2.39
SMT1-8	0.11	1.18	6.71	SMT3-2	0.23	5.36	2.41
SMT1-9	0.03	1.20	6.77	SMT3-3	0.07	5.47	2.46
SMT1-10	0.38	1.14	6.47	SMT3-4	0.17	5.41	2.43
SMT1-11	0.03	1.20	6.78	SMT3-5	0.03	5.50	2.47
SMT1-12	0.01	1.20	6.79	SMT3-6	0.06	5.48	2.46
SMT2-1	0.28	1.78	5.95	SMT3-7	0.25	5.35	2.40
SMT2-2	0.23	1.79	5.98	SMT3-8	0.11	5.45	2.45
SMT2-3	0.21	1.79	6.00	SMT3-9	0.03	5.50	2.47
SMT2-4	0.17	1.80	6.03	SMT3-10	0.38	5.26	2.36
SMT2-5	0.03	1.83	6.14	SMT3-11	0.03	5.50	2.47
SMT2-6	0.03	1.83	6.13	SMT3-12	0.02	5.51	2.47

Table 8

The [*a*] matrix of the SMT production line 1, 2, 5

Machine No.	$a_{j-starting}^{SMT1}$	$a_{j-Dormancy}^{SMT1}$	$a_{j-working}^{SMT1}$	Machine No.	$a_{j-starting}^{SMT1}$	$a_{j-Dormancy}^{SMT1}$	$a_{j-working}^{SMT1}$
SMT1-1	0	1	0	SMT2-7	0	0	0
SMT1-2	0	0	1	SMT2-8	1	0	1
SMT1-3	0	0	1	SMT2-9	0	0	1
SMT1-4	0	0	1	SMT2-10	0	1	0
SMT1-5	0	1	0	SMT2-11	0	0	1

Machine No.	$a_{j-starting}^{SMT1}$	$a_{j-Dormancy}^{SMT1}$	$a_{j-working}^{SMT1}$	Machine No.	$a_{j-starting}^{SMT1}$	$a_{j-Dormancy}^{SMT1}$	$a_{j-working}^{SMT1}$
SMT1-6	0	0	1	SMT2-12	0	0	0
SMT1-7	0	0	0	SMT3-1	0	1	0
SMT1-8	1	0	1	SMT3-2	0	1	0
SMT1-9	0	0	1	SMT3-3	0	0	0
SMT1-10	0	0	1	SMT3-4	0	1	0
SMT1-11	0	0	1	SMT3-5	0	1	0
SMT1-12	0	0	0	SMT3-6	0	1	0
SMT2-1	0	0	1	SMT3-7	0	1	0
SMT2-2	0	0	1	SMT3-8	0	1	0
SMT2-3	0	0	1	SMT3-9	0	1	0
SMT2-4	0	1	0	SMT3-10	0	1	0
SMT2-5	0	1	0	SMT3-11	0	1	0
SMT2-6	0	0	1	SMT3-12	0	1	0

According the formulas (17)-(28), the equipment, process and production line energy consumption are shown in Tables 9-11.

Table 9

Equipment energy consumption of each state of the SMT-x production line

	Starting, KWh	Dormancy, KWh	Working, KWh	Total consumption, KWh		Starting, KWh	Dormancy, KWh	Working, KWh	Total consumption, KWh
SMT x-1	9.63	0.93	55.81	66.37	SMT x-7	12.00	0.93	65.88	78.81
SMT x-2	6.07	0.93	42.91	49.91	SMT x-8	3.36	0.95	32.20	36.50
SMT x-3	1.07	0.95	20.23	22.25	SMT x-9	0.93	0.96	33.86	35.75
SMT x-4	4.00	0.94	31.29	36.23	SMT x-10	31.82	1.14	106.82	139.78
SMT x-5	0.18	0.60	10.17	10.94	SMT x-11	0.30	0.60	15.59	16.49
SMT x-6	0.43	0.96	16.93	18.32	SMT x-12	0.07	0.60	10.19	10.86

Table 10

Process energy consumption of automatic chip mounter & rail reflow soldering machine of line 1

Equipment	Real time power, KW	Starting, KWh	Dormancy, KWh	Working, KWh	Total energy consumption, Wh
Automatic Chip Mounter & Rail Reflow soldering	93.8KW	44.75	3.03	206.56	254.34

Table 11

Production line 1 energy consumption

Equipment	Real time power, KW	Starting, KWh	Dormancy, KWh	Working, KWh	Total energy consumption, KWh
SMT production line 1	77.6KW	69.84	10.48	441.88	522.20

5. Conclusion

In this paper, for the intelligent workshop, the energy consumption real-time sensing technology based on mutual inductance & a multi-granularity production line energy consumption modeling, do most of the work implement the energy consumption architecture. In device-level an AUBO-i5 is introduced to show the details of real-time sensing technology based on mutual inductance in standard loop and actual loop. Some key parameters, like nominal value of operation energy consumption, the percentage of the auxiliary energy consumption, and the operation energy efficiency coefficient, are obtained. Additionally, a multi-granularity production line energy consumption modeling based on SMT production lines is summarized for the workshop-level. Case studies are presented separately at the end of each section. Results show that the architecture can effectively sense and model the energy consumption of the devices and the workshop, which provides an available method for the fine management and control of energy consumption and energy efficiency.

As the first step in the whole project of the group, this study expects higher levels of workshop control such as the energy efficiency evaluation and the energy conservation optimization in the future study. While during the implementation of this study, it was concluded that:

1) In the workshop / production line, the energy consumption has a significant correlation with the operations. The frequent downtime and excessive waiting can both increase ineffective energy consumption, which can account for more than 30% of the total waste. Only by ensuring continuous and efficient scheduling of the production process can energy efficiency be effectively improved. The Advanced Planning and Scheduling (APS) and some evaluation index systems are needed.

2) The equipment energy consumption shows strong correlation with the control mode. The fundamental reason why the energy efficiency of same device under different control procedures given by different controller often varies greatly is that the existing control logic only aims to get a simple "set function" rather than "efficient, reliable, and low energy consumption function". In order to improve the energy efficiency of the equipment, the energy consumption constraints of control algorithm are essential.

This research has been partly applied in the AKM Co. Ltd. and in the near future, the authors hope it can be applied in some other discrete manufacturing industries or production line clusters. The group want to study the scenario application of blockchain in the energy consumption tracing and the digital twin in the energy saving control.

Acknowledgments

This work was financially supported the Ministry of education of Humanities and Social Science project (21YJCZH112 & 21YJA630111), the Changzhou Sci& Tech Program (CJ20210058 & CM20223014), the Fundamental Research Funds for the Central Universities (B220202027).

References

1. **Kimon, K.; Florian, F.; Ana, D. V.;** et al 2021. Global Energy and Climate Outlook 2021: Advancing Towards Climate Neutrality. Jrc Research Reports.
2. **Ye, W.; Wang, Y.** 2020. Energy efficiency evaluation of industrial heat exchangers based on fuzzy matter element method, Mechanika 26(2): 171-176. https://doi.org/10.5755/j01.mech.26.2.22848.
3. **Zheng, J.; Feng, G.; Ren, Z.;** et al 2022. China's energy consumption and economic activity at the regional level, Energy 259: 124948. https://doi.org/10.1016/j.energy.2022.124948.
4. **Ragab, A.; Ghezzaz, H.; Amazouz, M.** 2022. Decision fusion for reliable fault classification in energy-intensive process industries, Computers in Industry 138: 103640. https://doi.org/10.1016/j.compind.2022.103640.
5. **Jenny, L.; Ocampo-Martinez, C.** 2019. Energy efficiency in discrete-manufacturing systems: insights, trends, and control strategies, Journal of Manufacturing Systems 52(Part A): 131-145. https://doi.org/10.1016/j.jmsy.2019.05.002.
6. **Liu, F.; Wang, Q.** 2013. Energy efficiency assessment of mechanical manufacturing system: characteristics, state-of-the-art and future trends, China Mechanical Engineering 24(11): 1550-1557. https://doi.org/10.3969/j.issn.1004-132X.2013.11.025.
7. **He, Y.; Liu, F.; Cao, H**.; et al. 2007. Job scheduling model of machining system for green manufacturing, Chinese Journal of Mechanical Engineering 43(4): 21-28. https://doi.org/10.3321/j.issn:0577-6686.2007.04.005.
8. **Zhang, Z.; Wu, L.; Jis, S.** 2019. Energy consumption optimization for flexible job shop, Manufacturing Technology & Machine Tool 1(4): 162-168. https://doi.org/10.19287/j.cnki.1005-2402.2019.04.032.
9. **Jiang, M**. 2017. Energy saving scheduling for forging production [D]. Nanjing University of Science and Technology.
10. **Zhu, B.; Lu, H.; Bai, S.;** et al. 2016. Study on the charging combination optimization for forging production based on discrete shuffled frog leaping algorithm, Mechanika 22(5): 425-431. https://doi.org/10.5755/j01.mech.22.5.13191.
11. **Xie, J.; Cai, W.; Du, Y.;** et al. 2021. Modelling approach for energy efficiency of machining system based on torque model and angular velocity, Journal of Cleaner Production, 293(Feb.): 1-11. https://doi.org/10.1016/j.jclepro.2021.126249.
12. **Smith, L.; Ball, P.** 2012. Steps towards sustainable manufacturing through modelling material, energy and waste flows, International Journal of Production Economics 140(1): 227-238 https://doi.org/10.1016/j.ijpe.2012.01.036.
13. **Zhang, Y.; Li, L.; Liu, W.;** et al. 2022. Dynamics analysis and energy consumption modelling based on bond graph: taking the spindle system as an example. Journal of Manufacturing Systems 62: 539-549. https://doi.org/10.1016/j.jmsy.2022.01.009.
14. **He, Y.; Tian, X.; Li, Y.;** et al. 2022. Modeling and Analyses of energy consumption for machining features with flexible machining configurations, Journal of Manufacturing Systems 62: 463-476. https://doi.org/10.1016/j.jmsy.2022.01.001.
15. **Cai, W.; Liu, F.; Zhang, H.;** et al. 2017. Development of dynamic energy benchmark for mass production in machining systems for energy management and energy-efficiency improvement, Applied Energy 202(sep.15): 715-725. https://doi.org/10.1016/j.apenergy.2017.05.180.

F. Pei, Z. Li, W. Di, S. Mei, H. Song

REAL-TIME ENERGY CONSUMPTION SENSING SYSTEM IN SMT INTELLIGENT WORKSHOP

S u m m a r y

How to ensure the "carbon peaking and carbon neutrality" goal is a crucial problem for China with good performance, low cost and limited time. As a pillar industry, the manufacturing industry need offer more great potential helps. In this paper, for the intelligent workshop, firstly, an energy consumption architecture, based on mutual inductance sensing technology & a multi-granularity production line energy consumption modeling, is put forward. Secondly, the device-level sensing technology demonstrates the detailed implementation for the multi working condition machines whose power is unknown. And then, the research devoted the basic aspects of the proposed multi-granularity production line energy consumption modeling and summarized the implementation elements of 3-matrix (the attribute attributes, power attributes and cumulative timing attributes). Above the 2 sections, the robot and SMT production lines case studies are presented separately. Results show that the architecture can effectively sense and model the energy consumption of the devices and the workshop, which provides an available method for the fine management and control of energy consumption and energy efficiency. Through this study, we hope to provide some reference ideas for future researchers.

Keywords: real-time energy consumption, SMT intelligent workshop, 3-matrix.

Received August 24, 2022
Accepted October 9, 2023